Journal of Molecular Liquids 218 (2016) 625–631

Contents lists available at ScienceDirect

Journal of Molecular Liquids

journal homepage: www.elsevier.com/locate/molliq

Mechanistic investigation of Heck reaction catalyzed by new catalytic system composed of Fe_3O_4@OA–Pd and ionic liquids as co-catalyst

Ezzat Rafiee [a,b,*], Masoud Kahrizi [a]

[a] Faculty of Chemistry, Razi University, Kermanshah 67149, Iran
[b] Institute of Nano Science and Nano Technology, Razi University, Kermanshah 67149, Iran

ARTICLE INFO

Article history:
Received 4 October 2015
Received in revised form 9 February 2016
Accepted 17 February 2016
Available online xxxx

Keywords:
Polyoxometalate
Ionic liquid
Palladium
Nanocatalyst
Heck reaction
Hybrid compound

ABSTRACT

A simple and efficient protocol has been developed for the Heck coupling reaction catalyzed by a two component catalytic system composed of palladium deposited oleic acid coated-Fe_3O_4 nanoparticles (Fe_3O_4@OA–Pd) and thermo-regulated molybdovanadate-based ionic liquid salts ($H_5PMo_{10}V_2O_{40}$-IL, $Mo_{10}V_2$-IL) as a novel and recyclable catalytic system. In this system, low amounts of $Mo_{10}V_2$-ILs are used as an efficient co-catalyst, which reduce cost and increase efficiency in the Heck coupling reaction. These thermo-regulated co-catalysts are thermo-responsive, and could reversibly transform to precipitate with a decrease in temperature. In this study, the catalytic activities of various types of $Mo_{10}V_2$-IL including $Mo_{10}V_2$-(3-sulfonic acid) propylpyridine ($Mo_{10}V_2$-PyPS), $Mo_{10}V_2$-(4-sulfonic acid) butylpyridine ($Mo_{10}V_2$-PyBS), $Mo_{10}V_2$-(4-sulfonic acid) butyltrimethyl amine ($Mo_{10}V_2$-TMABS), $Mo_{10}V_2$-(4-sulfonic acid) butyltriethyl amine ($Mo_{10}V_2$-TEABS) and $Mo_{10}V_2$-(4-sulfonic acid) butyltributyl amine ($Mo_{10}V_2$-TBABS) were investigated in the Heck reaction. It was shown that all of the mentioned co-catalysts are efficient. It is apparent from cyclic voltammetric measurements that, these catalytic systems are electroactive and undergo reversible redox transitions between palladium nanoparticles and $Mo_{10}V_2$-IL species, also, it contains strong acid sites and mobile protons which can activate Ar–X and Pd–X bonds in oxidative addition and reductive elimination steps. As evidenced from mechanistic investigations, the electron transfer properties and Brönsted acidity of $Mo_{10}V_2$-ILs have been most pronounced upon application of the Fe_3O_4@OA–Pd and $Mo_{10}V_2$-IL system in the Heck coupling reaction. Fe_3O_4@OA–Pd and $Mo_{10}V_2$-PyPS exhibited excellent activities and the methodology is applicable to diverse substrates providing good to excellent yields of desired products. Moreover, this catalytic system was recycled for four consecutive cycles without any significant loss in activity.

1. Introduction

Palladium-catalyzed arylation of olefins, known as the Heck reaction, is one of the most important reactions for the formation of C—C bonds in organic synthesis, from both the research and industrial points of view [1–5]. Because of its tolerance to different functional groups, a variety of applications in the synthesis of pharmaceuticals, fine chemicals, polymers and natural compounds have been worked out [6,7]. Despite the importance of palladium catalyzed Heck reaction, the homogeneous palladium-based catalysis has significant drawbacks including low catalyst stability, possible toxicity caused by residual metal species, and inability in catalyst recovery, which have impeded their large scale application in industry. Moreover, the homogeneous palladium catalysts tend to lose their catalytic activity because of palladium metal aggregation and precipitation [8,9]. Nowadays, the chemists have been interested in the development of different aspects of palladium catalysts by deposition of palladium on solid supports [10–17].

Palladium-supported catalysts mimic their homogeneous counterparts and can be considered as 'soluble' analogues since they are readily dispersed and exhibit an intrinsically high surface area, an attribute that allows excellent accessibility of substrates to the surface bound active catalytic sites. Magnetic nanoparticles (MNPs) as catalyst supports have been attracting more and more attention because they can be easily recovered from the reaction mixture simply by using an external magnet, thus eliminating the necessity of tedious centrifugation, filtration, or membrane separation steps [18–20]. Fe_3O_4 nanoparticles are reactive especially in an acidic environment and thereby lose their magnetic properties. Oleic acid (OA) as a protecting shell can be utilized to coat the Fe_3O_4 nanoparticles to form a core–shell (Fe_3O_4@OA) structure. Meanwhile, the OA shell can prevent the aggregation of the Fe_3O_4 particles and provide numerous double bonds for location of palladium nanoparticles on the core–shell structure [21].

---

* Corresponding author at: Faculty of Chemistry, Razi University, Kermanshah 67149, Iran.
E-mail addresses: e.rafiei@razi.ac.ir, Ezzat_rafiee@yahoo.com (E. Rafiee).

http://dx.doi.org/10.1016/j.molliq.2016.02.055

Recently, catalytic systems which contain ionic liquids (ILs) have received much attention as promising green catalysts to reuse homogeneous catalysts [22–24]. Ionic liquids are normally composed of relatively large organic cations and inorganic or organic anions and have attracted a lot of interest for their unique properties, such as negligible volatile pressure, low toxicity, very low flammability, and the ability to dissolve in many organic and inorganic solvents [25]. The combination of organic cation parts with polyoxometalates (POMs) can cause the formation of POM-based ionic liquids (POM-ILs) that are emerging to be very important in catalysis [26–29]. These interesting organic–inorganic hybrid materials have properties of both POM anion and IL cation. POM-ILs with electron transfer ability and Brönsted acid property [30–32] can act as excellent co-catalyst and strong activator for reactants in coupling reactions. Despite the advantages of ILs, there exist some drawbacks about catalysis with IL based systems: high solubility in most of solvents producing separation problems which is an important restriction for catalytic systems. One of the main ways to overcome this problem is the use of thermo-regulated IL which can convert from homogeneous to heterogeneous form by reducing temperature.

In order to continue our studies directed towards the development of practical procedures for some important transformations [33–36], we developed new efficient catalytic systems composed of a family of POM-ILs (Scheme 1). These catalysts incorporate (3-sulfonic acid) propylpyridine (PyPS), (4-sulfonic acid) butylpyridine (PyBS), (4-sulfonic acid) butyltrimethyl amine (TMABS), (4-sulfonic acid) butyltriethyl amine (TEABS) and (4-sulfonic acid) butyltributyl amine (TBABS) as cations and $H_5PMo_{10}V_2O_{40}$ ($Mo_{10}V_2$) as anion and palladium deposited oleic acid coated-Fe_3O_4 nanoparticles (Fe_3O_4@OA–Pd). These catalytic systems were employed in the Heck coupling reaction. All of these catalytic systems exhibited remarkable activities in a model reaction and the systems tolerate a wide variety of aryl halide compounds and styrene with good to excellent yields of desired products. Also the effect of redox properties and Brönsted acidity of POM-ILs part of mentioned catalytic system were investigated.

2. Experimental

2.1. General remarks

All of the reagents and solvents were commercially available and purchased from Fluka, Merck, and Aldrich chemical companies. FT-IR spectra were recorded with KBr pellets using a Bruker ALPHA FT-IR spectrometer. UV–vis spectra were obtained with an Agilent (8453) UV–vis diode-array spectrometer using quartz cells of 1 cm optical path. The potential variation was measured with a Hanna 302 pH meter. Thin layer chromatography (TLC) on precoated silica gel Fluorescent 254 nm (0.2 mm) on an aluminum plate was used for monitoring the reactions. The cross coupling products were characterized by their ^1H NMR spectra. The electrochemical reduction of catalyst was studied in phosphate buffer (0.1 M), pH = 7. A glassy carbon electrode was used as the working electrode and Ag/AgCl as the reference electrode. Cyclic voltammograms (ν, 0.1 V s^{-1}) were obtained at ambient temperature (20 ± 5 °C).

2.2. Preparation of $Mo_{10}V_2$

$Mo_{10}V_2$ was prepared according to the following procedure: sodium metavanadate (24.4 g) was dissolved by boiling in 100 mL of water and then mixed with 7.1 g of Na_2HPO_4 in 100 mL of water. Then this solution was cooled, 5 mL of concentrated sulfuric acid was added, and the solution developed a red color. An addition of 121.0 g of $Na_2MoO_4 \cdot 2H_2O$ dissolved in 200 mL of water was then made. While the solution was vigorously stirred, 85 mL of concentrated sulfuric acid was added slowly, and the hot solution was allowed to be cooled to room temperature. $Mo_{10}V_2$ was then extracted with 500 mL of diethyl ether. Evaporation of the solvent afforded a crude product which dissolved in water, concentrated to first crystal formation, and then allowed to crystallize further. The large red crystals that formed were filtered, washed with water, and air dried [37].

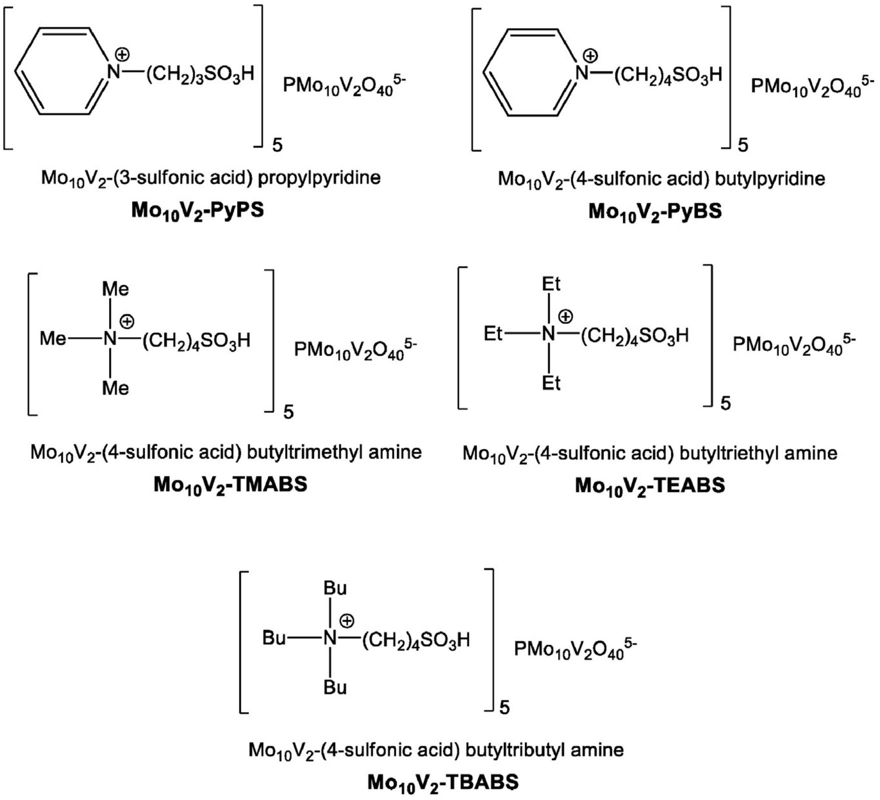

Scheme 1. Structures of organic–inorganic hybrid compounds (POM-ILs).

2.3. Synthesis of $Mo_{10}V_2$-IL catalysts

For the preparation of $Mo_{10}V_2$-IL cations, their respective amine (pyridine, trimethyl amine, triethyl amine and tributyl amine) (0.11 mol) and 1,3-propanesultone or 1,4-propanesultone (0.10 mol) were dissolved in toluene (30 mL) and stirred at 40 °C for 72 h under nitrogen atmosphere. The produced precipitate was filtered, washed with diethyl ether three times and dried in vacuum. For the preparation of POM-IL, the prepared cation (0.1 mol) was added to an aqueous solution of $Mo_{10}V_2$ (0.02 mol, 5 mL), and then the mixture was stirred at room temperature for 24 h. Water was removed in vacuum to give the final product as a solid.

2.4. Synthesis of oleic acid coated-Fe_3O_4 nanoparticles

The oleic acid coated-Fe_3O_4 nanoparticles were prepared by a co-precipitation method, according to a synthesis route described in our previous publication [38]. Typically, $FeCl_2 \cdot 4H_2O$ (4.3 g) and $FeCl_3 \cdot 6H_2O$ (11.6 g) were mixed with 350 mL of deionized water. The resulting solution was heated to 80 °C while stirring, vigorously. Then, 20 mL of 25% NH_4OH was quickly added into the solution. The resulting suspension was vigorously stirred for 5 min and then, 1 mL oleic acid was added into the suspension. After mixing for 25 min, the black precipitates were collected with the help of a magnet and washed repeatedly with deionized water and ethanol, then dried at vacuum conditions.

2.5. Synthesis of Fe_3O_4@OA–Pd catalyst

A solution of $Na_2[PdCl_4]$ (0.011 M) in ethanol was prepared by reacting $PdCl_2$ (0.50 g, 2.82 mmol) and NaCl (0.33 g, 5.64 mmol) at room temperature. Fe@OA nanoparticle (0.5 g in 700 mL methanol) solution was held at 25 °C for 1 h and then $Na_2[PdCl_4]$ (100 mL, 0.011 M) was added. Then 100 mL of NaOAc (5 M) was added rapidly into the solution. After that, 50 mL of methanol was added, and the product was separated by a magnetic field, washed with ethanol and water three times and dried at vacuum conditions [38].

2.6. General procedure for the Heck coupling reaction

For Heck coupling reaction, a reaction tube was charged with aryl halide (4 mmol), styrene (4 mmol), tetrabutylammonium bromide, TBAB (4 mmol), Fe@OA–Pd (0.38 mol%), $Mo_{10}V_2$-IL (0.26 mol%) and 5 mL DMF and the resulting mixture was refluxed at 120 °C under a dry nitrogen atmosphere for appropriate time. Progress of the reaction was monitored by TLC. Upon completion of the reaction, Fe@OA–Pd was separated by magnet, washed with diethyl ether (2 × 10 mL) and water (2 × 10 mL), and then dried under vacuum for reusing. Also the reaction mixture was then cooled to 5 °C and $Mo_{10}V_2$-IL was separated by filtration, and washed with diethyl ether (3 × 10 mL) and dried under vacuum for reusing. The residual mixture was extracted by CH_2Cl_2 (3 × 20 mL), and the combined organic layers were dried over $MgSO_4$. Solvent was evaporated and the crude product was characterized by ^1H NMR spectroscopy [38].

3. Results and discussion

In continuation of our studies about the effect of POMs on the coupling reactions [36], we decided to investigate the role of another forms of POMs, ionic liquid forms, in these types of organic reactions. $Mo_{10}V_2$ is soluble in most of polar organic solvents, and cannot be used as a catalyst here. On the other hand, $Mo_{10}V_2$ based pyridinium or ammonium sulfonic group ILs have some significant physical properties such as reversible thermal response. Therefore, we believe that this type of ILs can be applied as an efficient and recyclable part of our proposed catalytic system in coupling reactions especially in the Heck reaction.

In the first step of our investigations, we prepared Fe_3O_4@OA–Pd and a series of $Mo_{10}V_2$-ILs with different IL parts, and their structural

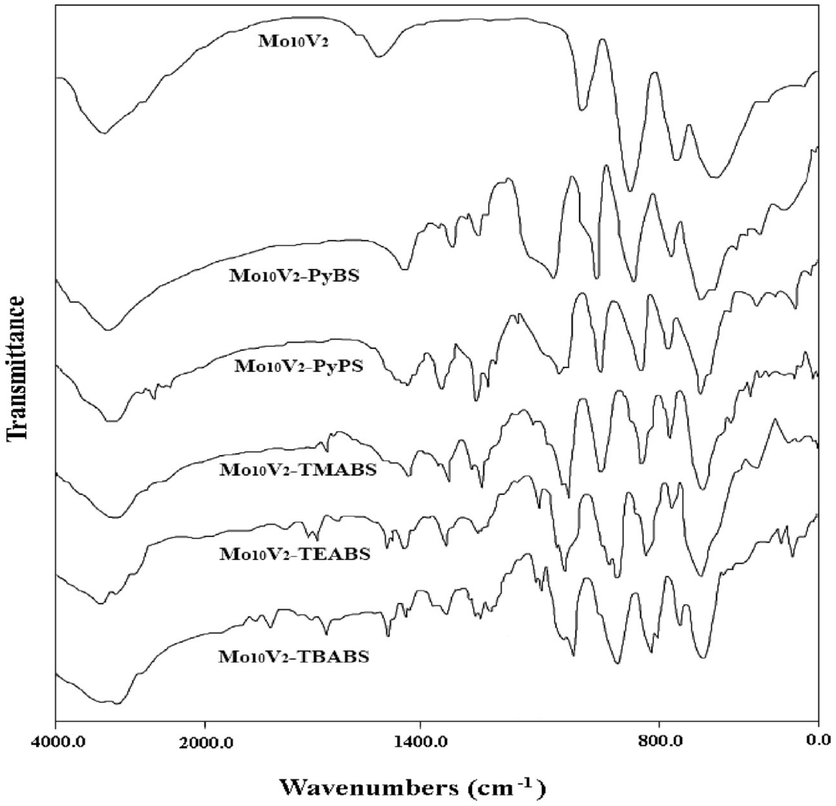

Fig. 1. FT-IR spectra of different $Mo_{10}V_2$-ILs.

Table 1
Comparison of activity of $Mo_{10}V_2$-IL series in the Heck reaction.[a]

Entry	POM-IL	Time (h)	Yield (%)	TON
1	–	24	0	0
2	$Mo_{10}V_2$-PyPS	12	94	500
3	$Mo_{10}V_2$-PyBS	16	88	468
4	$Mo_{10}V_2$-TMABS	18	81	430
5	$Mo_{10}V_2$-TEABS	24	92	489
6	$Mo_{10}V_2$-TBABS	24	82	436

[a] Reaction conditions: styrene (4 mmol), 1-bromobenzene (4 mmol), Fe_3O_4@OA–Pd (0.19 mol%), $Mo_{10}V_2$-IL (0.13 mol%), TBAB (4 mmol) and at 120 °C.

features were investigated using FT-IR and TEM techniques (Supplementary information, Figs. S1 and S2).

TEM observations and FT-IR spectrum indicated that Fe_3O_4@OA–Pd as a main catalyst in this catalytic system has a uniform morphology. According to the FT-IR spectrum of Fe_3O_4@OA–Pd, the broad band near 3446 cm^{-1} refers to the OH stretching vibration associated with absorbed water molecule. Two bands at around 2919 and 2854 cm^{-1} were attributed to the asymmetric and symmetric stretching of CH_2 groups of oleic acid, respectively. The peak at 1641 cm^{-1} exhibited the presence of the CC stretching vibration. Meanwhile, two new bands at 1404 and 1542 cm^{-1} appeared which are characteristic of the asymmetric –(COO) and the symmetric –(COO) stretch vibration band, respectively. The absorption band at 583 cm^{-1} was attributed to Fe—O stretch vibrations which confirm the existence of Fe_3O_4 nanoparticles. Other characterization results have been presented in our previous publication[21].

Also The FT-IR spectra of $Mo_{10}V_2$-ILs are shown in Fig. 1. As shown in Fig. 1, the structures of all $Mo_{10}V_2$-ILs were confirmed.

Next we decided to study the roles of $Mo_{10}V_2$-IL series in the Heck reaction. Initially, we compared the catalytic performances of Fe_3O_4@OA–Pd and different $Mo_{10}V_2$-ILs in the reaction of styrene with 1-bromobenzene as model reaction. As seen in Table 1, in the absence of the $Mo_{10}V_2$-IL the reaction did not proceed even after 24 h. The results showed that all of the listed catalytic systems can catalyze the reaction in a desirable manner and the corresponding product was obtained in good to excellent yield but in different reaction times.

POMs can affect on the reactions with two different mechanisms: Brönsted acid and electron transfer mechanism. In order to probe which one is the main mechanism, the acidity of $Mo_{10}V_2$-ILs and cyclic voltammetry measurements of $Mo_{10}V_2$-PyPS, Fe_3O_4@OA–Pd and mixture of both catalysts were investigated.

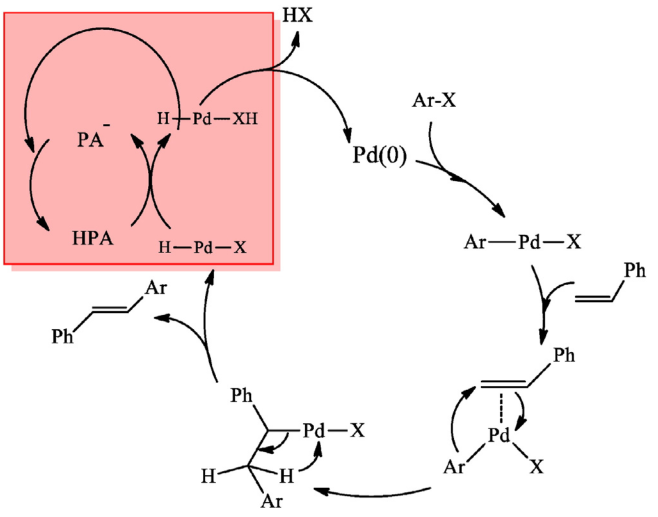

Scheme 2. Proposed mechanism for Heck reaction catalyzed by Fe_3O_4@OA–Pd and $Mo_{10}V_2$-ILs, HPA (heteropoly acid) and PA^- (polyoxoanion).

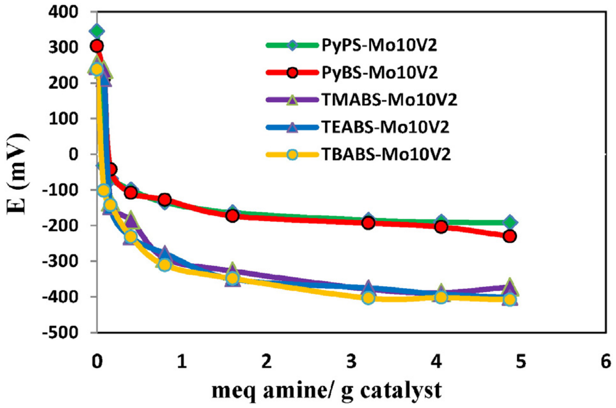

Fig. 2. Potentiometric titration curves of $Mo_{10}V_2$-IL series.

Considering that the Heck reaction is affected by acidity of the catalyst, the acidity of the $Mo_{10}V_2$-ILs plays an important role in this transformation. It seems that $Mo_{10}V_2$-ILs can act as bond activator in

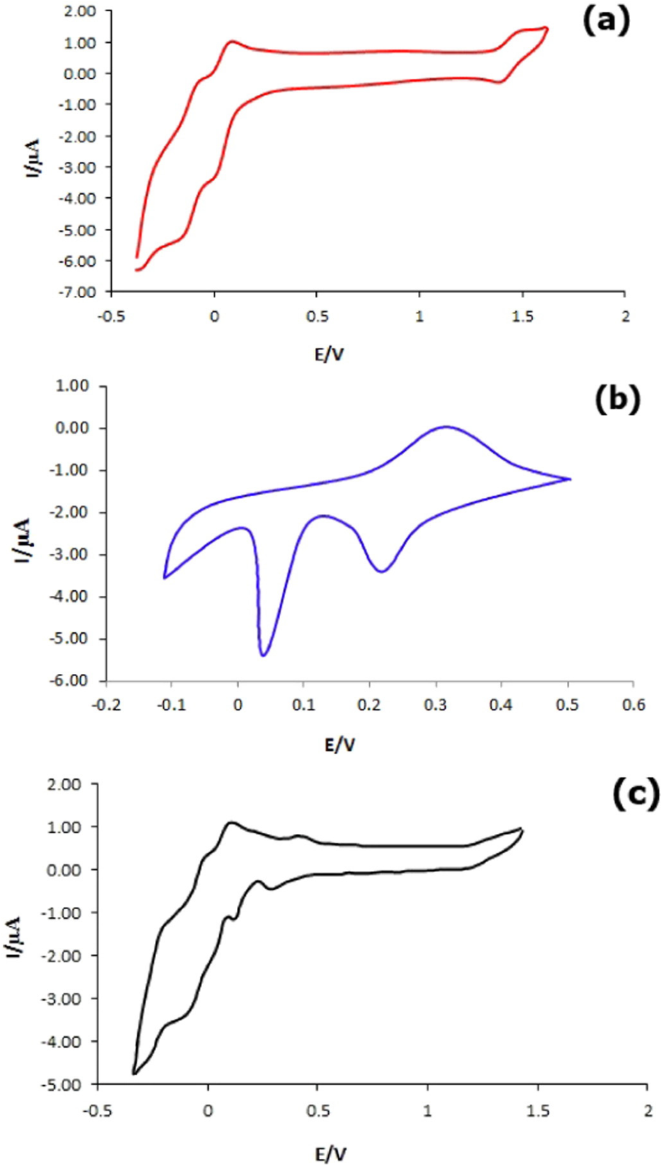

Fig. 3. Cyclic voltammograms of a) $Mo_{10}V_2$-PyPS, b) Fe_3O_4@OA–Pd and c) mixture of both modified glassy carbon electrode in a phosphate buffer solution of pH = 7, 100 mV/s.

Table 2
Electrochemical data.

Catalyst	E_{Pc} (V)	E_{Pa} (V)	Potential shift		Assignment peak
			ΔE_{Pc} (V)	ΔE_{Pa} (V)	
Fe_3O_4@OA–Pd	+0.30	+0.21	–		Fe(II)/Fe(III)
	N.A.	+0.03	–		Pd(0)/Pd(II)
$Mo_{10}V_2$-PyPS	+1.46	+1.42	–		V(IV)/V(V)
	+0.07	+0.00	–		Mo(IV)/Mo(III)
	−0.07	−0.14	–		Mo(V)/Mo(IV)
Mixture of both components	+1.30	+1.23	−0.16	−0.19	V(IV)/V(V)
	+0.40	+0.28	+0.10	+0.07	Fe(II)/Fe(III)
	N.A.	+0.1	N.A.	+0.07	Pd(0)/Pd(II)
	+0.10	+0.02	+0.03	+0.02	Mo(IV)/Mo(III)
	−0.03	−0.12	+0.04	+0.02	Mo(V)/Mo(IV)

oxidative addition and reductive elimination steps in the Heck reaction. A possible mechanism for the Heck reaction in the presence of Fe_3O_4@OA–Pd and $Mo_{10}V_2$-ILs is proposed in Scheme 2. In the first step the C–X bond of an aryl halide (X = Br, Cl) is oxidatively added to the palladium atom. At this point, the oxidation of palladium (0) is facilitated by $Mo_{10}V_2$-ILs. Palladium then forms a π complex with the alkene and next, the alkene inserts itself in the palladium–carbon bond (Pd—Ar). In the next step, β-hydride elimination causes the formation of a new palladium–alkene π complex. Finally this complex is destroyed and the desired product is released. As shown in the highlighted part of Scheme 2, in the reductive elimination step, the Pd–X bond is activated by $Mo_{10}V_2$-IL acidic hydrogens. H–X is a very good leaving group and this intermediate is very susceptible to loss of H–X group. Finally, in the reductive elimination step a formed polyoxoanion with taking hydrogen in Pd—H group returns to acidic form and palladium reduces to palladium (0). Further research is under investigation in our laboratory.

The difference of IL parts in $Mo_{10}V_2$-IL series, apparently influenced the acidity of the $Mo_{10}V_2$-ILs, which was probed by a potentiometric titration with an organic base [38].

As shown in Fig. 2, all kinds of $Mo_{10}V_2$-ILs presented very strong acid sites, $Ei > 100$ mV. The presence of pyridine as an electron withdrawing group in $Mo_{10}V_2$-IL structures was accompanied by a gradual increase in acidic strength active sites. Strength of acidic sites of different hybrid materials is as the following trends: PyPS-$Mo_{10}V_2$ > PyBS-$Mo_{10}V_2$ > TMABS-$Mo_{10}V_2$ > TEABS-$Mo_{10}V_2$ > TBABS-$Mo_{10}V_2$ (*Ei* values for these compounds are 345, 303, 253, 245, and 238 mV respectively). As a result, it seems that higher activity of $Mo_{10}V_2$-PyPS is related to higher acidic strength of this catalyst because the number of acidic sites in all kinds of co-catalyst is approximately similar.

In order to probe the electron transfer behavior of $Mo_{10}V_2$-ILs and Fe_3O_4@OA–Pd, we decided to investigate this property of $Mo_{10}V_2$-ILs and Fe_3O_4@OA–Pd by means of cyclic voltammetry (CV) measurements. The CV responses of $Mo_{10}V_2$-PyPS, Fe_3O_4@OA–Pd and mixture of both component modified glassy carbon electrode in a phosphate buffer solution of pH = 7 are shown in Fig. 3. In the potential range between E = −0.34 and E = +1.58 V, three pairs of redox peaks were observed for $Mo_{10}V_2$-PyPS modified electrode (Fig. 3a). It can be attributed to the electron-transfer reaction of Mo(V)/Mo(IV), Mo(IV)/Mo(III) and V(IV)/V(V) couples. Also, the oxidation behavior of Fe_3O_4@OA–Pd was investigated by means of CV and the oxidation of Pd(0)/Pd(II) was identified with its characteristic peak located at E = +0.03 V (Fig. 3b) [39, 40]. The peaks at potential 0.16–0.42 are attributed to Fe(II)/Fe(III) nanocrystals [41]. In addition, to explore the interaction between Fe_3O_4@OA–Pd and $Mo_{10}V_2$-IL, we investigate the CV of mixed Fe_3O_4@OA–Pd and $Mo_{10}V_2$-IL glassy carbon electrode. As shown in Fig. 3c, in the potential range between E = −0.33 and E = +1.42 V, all the redox peaks of $Mo_{10}V_2$-PyPS and Fe_3O_4@OA–Pd were observed. Also the shift in the potential of characteristic peak of Fe_3O_4@OA–Pd and $Mo_{10}V_2$-PyPS in glassy carbon electrode, clearly indicates the interaction between Fe_3O_4@OA–Pd and $Mo_{10}V_2$-PyPS. The amount of the shifts in different peaks is reported in Table 2.

To establishing the best reaction conditions, firstly the model reaction was carried out in the absence of the $Mo_{10}V_2$-PyPS, the reaction did not proceed at all and the starting materials were remained intact after 24 h (Table 3, entry 1). Increasing the quantity of $Mo_{10}V_2$-PyPS from 0.13 mol% to 0.26 mol% decreases the reaction time but more than this amount had no significant effect on the reaction time and yield (entries 2–4). Improvement in time of the reaction was observed as the quantity of Fe_3O_4@OA–Pd as catalyst was increased from 0.188 mol% to 0.376 mol%. Further increasing in the Fe_3O_4@OA–Pd quantity showed no improvement in the yield or reaction time (entries 4–6). Therefore, 0.26 mol% of the $Mo_{10}V_2$-PyPS and 0.38 mol% of Fe_3O_4@OA–Pd were chosen as the optimum amounts of the catalytic system for further reactions. Moreover the effects of various solvents, such as H_2O, dimethylacetamide (DMAc), toluene and DMF have been studied (Table 3, entries 5, 7–9). DMF at 120 °C is found to be the choice in terms of yield and reaction time (entry 5).

This catalytic system is efficient for a variety of aromatic bromides and chlorides (Table 4). The results showed acceptable yields of the corresponding products using aryl bromides with electron-rich or electron-poor substituents, except in the case of 4-bromoaniline and 4-chloroaniline, where 43 and 56% yields were obtained (entries 3, 7). Most reactions using styrene and aryl bromides gave well to excellent yields regardless of steric effect of the substrates. This catalytic system showed high selectivity for the *trans*-configured products in all cases, and no *cis*/*gem* olefin products were observed.

As expected, reactions with aryl chlorides gave slightly lower yields and higher reaction time leaving some unreacted starting materials. It should be noted that, aryl halides containing electron-withdrawing functional groups give higher yields with lower reaction times compared to those containing electron-donating functional groups.

Table 3
Effect of the POM on the Heck coupling reaction.[a]

Entry	Catalyst		Solvent	Time (h)	Yield (%)[b]	TON
	Fe_3O_4@OA–Pd (mol%)	$Mo_{10}V_2$-IL				
1	0.19	–	DMF	24	0	0
2	0.19	$Mo_{10}V_2$-PyPS (0.13 mol%)	DMF	12	94	500
3	0.19	$Mo_{10}V_2$-PyPS (0.26 mol%)	DMF	9	89	473
4	0.19	$Mo_{10}V_2$-PyPS (0.39 mol%)	DMF	9	93	494
5	0.38	$Mo_{10}V_2$-PyPS (0.26 mol%)	DMF	7	96	251
6	0.56	$Mo_{10}V_2$-PyPS (0.26 mol%)	DMF	7	90	159
7	0.38	$Mo_{10}V_2$-PyPS (0.26 mol%)	H_2O	24	32	85
8	0.38	$Mo_{10}V_2$-PyPS (0.26 mol%)	Toluene	24	8	21
9	0.38	$Mo_{10}V_2$-PyPS (0.26 mol%)	DMAc	24	78	207

[a] Reaction conditions: styrene (4 mmol), bromobenzene (4 mmol), TBAB (4 mmol) at 120 °C.
[b] Isolated yield.

Table 4
Heck reaction of various aryl halides with styrene.

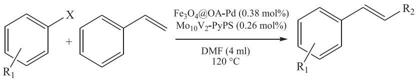

Entry	Aryl halide	Time (h)	Yield (%)[a]	TON
1	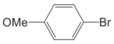	12	74	197
2	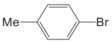	12	88	234
3	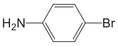	24	43	114
4	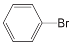	7	96	255
5	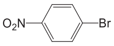	4	94	250
6	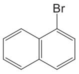	6	86	229
7	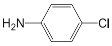	24	56	149
8	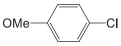	24	66	175
9	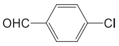	12	87	231
10	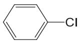	12	81	216
11	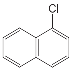	12	83	221
12	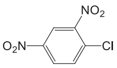	8	97	258

[a] Isolated yield, all products were characterized by comparison of their spectroscopic data with those reported in the literature [21, 42–44].

An important factor in the development of solid acids for most of the organic reactions is the reusability of the catalysts. This aspect was considered by recovering of the Fe_3O_4@OA–Pd after each catalytic run by magnet and reusing it in a new cycle. But in the case of $Mo_{10}V_2$-PyPS, considering that this catalyst is insoluble in the reaction medium at 5 °C, the catalyst can be recovered easily by simple filtration.

In order to evaluate the reusability of our catalytic system, a control test was performed using 0.04 g of the first recycled catalysts (primeval amount of catalytic system) and 92% yield of the product was obtained after 12 h. As shown in Fig. 4, the catalytic system revealed a remarkable activity and was reused up to at least four consecutive cycles without appreciable reduction in the catalytic activity of the catalyst.

4. Conclusion

In conclusion, we have developed an efficient protocol for the Heck coupling reaction using Fe_3O_4@OA–Pd and $Mo_{10}V_2$-ILs as efficient, heterogeneous and recyclable catalytic systems. The reaction was carried out in base and ligand free conditions and could be employed for the condensation of different aryl halides and styrene. Our investigation

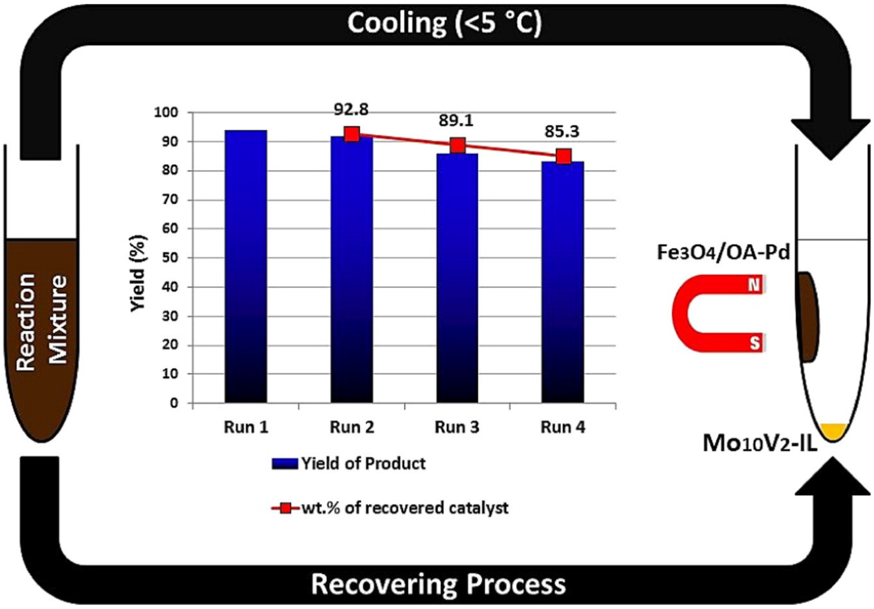

Fig. 4. Reusability of Fe_3O_4@OA–Pd and $Mo_{10}V_2$-PyPS in the model reaction (after 12 h).

on the role of $Mo_{10}V_2$-ILs in this study demonstrated that, these co-catalysts can influence the Heck reaction in two different and simultaneous manners: Brönsted acid and electron transfer pathways which make it a highly efficient co-catalyst for this type of organic transformation. Moreover, the recovery of this system consists of a single filtration for $Mo_{10}V_2$-ILs albeit after cooling to 5 °C and magnetic separation for Fe_3O_4@OA–Pd. Both components of this catalytic system are stable under the present reaction conditions and after separation from reaction media, can be used up to four catalytic cycles without significant loss in activity. Further studies on extending the application of this catalytic system in other organic synthesis are ongoing in our laboratory.

Acknowledgment

The authors thank the Razi University Research Council for the support of this work.

Appendix A. Supplementary data

TEM image and FT-IR spectrum of Fe_3O_4@OA–Pd are available. Supplementary data associated with this article can be found in the online version, at http://dx.doi.org/10.1016/j.molliq.2016.02.055.

References

[1] R.F. Heck, J.P. Nolley, J. Organomet. Chem. 37 (1972) 2320–2322.
[2] I.P. Beletskaya, A.V. Cheprakov, Chem. Rev. 100 (2000) 3009–3066.
[3] M. Shibasaki, E.M. Vogl, J. Organomet. Chem. 576 (1999) 1–15.
[4] J. Mo, L. Xu, J. Ruan, S. Liu, J. Xiao, Chem. Commun. (2006) 3591–3593.
[5] W.A. Herrmann, C. Brössmer, K. Öfele, C.P. Reisinger, Angew. Chem. Int. Ed. 34 (1995) 1844–1848.
[6] C.Y. Hong, N. Kado, L.E. Overman, J. Am. Chem. Soc. 115 (1993) 11028–11029.
[7] Y. Chang, G. Wu, G. Agnel, E.-I. Negishi, J. Am. Chem. Soc. 112 (1990) 8589–8590.
[8] M.T. Reetz, J.G. de Vries, Chem. Commun. (2004) 1559–1563.
[9] D. Astruc, Inorg. Chem. 46 (2007) 1884–1894.
[10] H. Hagiwara, Y. Shimizu, T. Hoshi, T. Suzuki, M. Ando, K. Ohkubo, C. Yokoyama, Tetrahedron Lett. 42 (2001) 4349–4351.
[11] N. Iranpoor, H. Firouzabadi, S. Motevalli, M. Talebi, J. Organomet. Chem. 708-709 (2012) 118–124.
[12] N. Iranpoor, H. Firouzabadi, A. Safavi, S. Motevallia, M.M. Doroodmand, Appl. Organomet. Chem. 26 (2012) 417–424.
[13] B. Tamami, S. Ghasemi, J. Mol. Catal. A Chem. 322 (2010) 98–105.
[14] K.S.A. Vallin, P. Emilsson, M. Larhed, A. Hallberg, J. Organomet. Chem. 67 (2002) 6243–6246.
[15] L. Xu, W. Chen, J. Ross, J. Xiao, Org. Lett. 3 (2001) 295–297.
[16] Y. Uozumi, T. Watanabe, J. Organomet. Chem. 64 (1999) 6921–6922.
[17] L. Wang, Y. Zhang, Ch. Xie, Y. Wang, Synlett 12 (2005) 1861–1864.
[18] A. Hu, G.T. Yee, W.B. Lin, J. Am. Chem. Soc. 127 (2005) 12486–12487.
[19] N.T.S. Phan, C.S. Gill, J.V. Nguyen, Z.J. Zhang, C.W. Jones, Angew. Chem. Int. Ed. 45 (2006) 2209–2211.
[20] R. Abu-Reziq, H. Alper, D. Wang, M.L. Post, J. Am. Chem. Soc. 128 (2006) 5279–5282.
[21] E. Rafiee, A. Ataei, Sh. Nadri, M. Joshaghani, S. Eavani, Inorg. Chim. Acta 409 (2014) 302–309.
[22] Y. Leng, J. Wang, D. Zhu, X. Ren, H. Ge, L. Shen, Angew. Chem. Int. Ed. 48 (2009) 168–171.
[23] M.V. Khedkar, T. Sasaki, B.M. Bhanage, ACS Catal. 3 (2013) 287–293.
[24] J. Chen, G. Zhao, L. Chen, RSC Adv. 4 (2014) 4194–4202.
[25] T.L. Greaves, C.J. Drummond, Chem. Rev. 108 (2008) 206–237.
[26] Y. Leng, H. Ge, C. Zhou, J. Wang, Chem. Eng. J. 145 (2008) 335–339.
[27] X. Chen, B. Souvanhthong, H. Wang, H. Zhang, X. Wang, M. Huo, Appl. Catal. B: Environ. 138-139 (2013) 161–166.
[28] W. Zhang, Y. Leng, D. Zhu, Y. Wu, J. Wang, Catal. Commun. 11 (2009) 151–154.
[29] Y. Leng, J. Wang, D. Zhu, Y. Wu, P. Zhao, J. Mol. Catal. A Chem. 313 (2009) 1–6.
[30] H. Liu, P. He, Z. Li, C. Sun, L. Shi, Y. Liu, G. Zhu, J. Li, Electrochem. Commun. 7 (2005) 1357–1363.
[31] Y. Ding, W. Zhao, J. Mol. Catal. A Chem. 337 (2011) 45–51.
[32] Y. Leng, J. Wang, D.R. Zhu, Y.J. Wu, P.P. Zhao, J. Mol. Catal. A Chem. 313 (2009) 1–6.
[33] E. Rafiee, S. Eavani, Catal. Commun. 25 (2012) 64–68.
[34] E. Rafiee, M. Khodayari, M. Kahrizi, R. Tayebee, J. Mol. Catal. A Chem. 358 (2012) 121–128.
[35] E. Rafiee, S. Eavani, B. Malaekeh-Nikouei, Chem. Lett. 41 (2012) 438–440.
[36] E. Rafiee, M. Kahrizi, Res. Chem. Intermed. (2015), http://dx.doi.org/10.1007/s11164-015-2077-3 (in press).
[37] G.A. Tsigdinos, C.J. Hallada, Inorg. Chem. 7 (1968) 437–441.
[38] E. Rafiee, M. Joshaghani, S. Eavani, S. Rashidzadeh, Green Chem. 10 (2008) 982–989.
[39] R.N. Biboum, B. Keita, S. Franger, C.H.P. Nanseu Njiki, G. Zhang, J. Zhang, T. Liu, I. Martyr Mbomekalle, L. Nadjo, Materials 3 (2010) 741–754.
[40] P. Bertoncello, M. Peruffo, P.R. Unwin, Chem. Commun. (2007) 1597–1599.
[41] L. Li, Y. Dou, L. Wng, M. Luo, J. Liang, RSC Adv. 4 (4) (2014) 25658–25665.
[42] N. Nowrouzi, D. Tarokh, S. Motevalli, J. Mol. Catal. A Chem. 385 (2014) 13–17.
[43] L. Botella, C. Najera, Tetrahedron Lett. 45 (2004) 1833–1836.
[44] K.M. Dawood, Tetrahedron 63 (2007) 9642–9651.